Magnetic polarons in a nonequilibrium polariton condensate

Paweł Miętki and Michał Matuszewski
Institute of Physics, Polish Academy of Sciences, Al. Lotnikow 32/46, PL-02668 Warsaw, Poland
(Received 18 July 2017; published 25 September 2017)

We consider a condensate of exciton polaritons in a diluted magnetic semiconductor microcavity. Such a system may exhibit magnetic self-trapping in the case of sufficiently strong coupling between polaritons and magnetic ions embedded in the semiconductor. We investigate the effect of the nonequilibrium nature of exciton polaritons on the physics of the resulting self-trapped magnetic polarons. We find that multiple polarons can exist at the same time, and we derive a critical condition for self-trapping that is different from the one predicted previously in the equilibrium case. Using the Bogoliubov–de Gennes approximation, we calculate the excitation spectrum and provide a physical explanation in terms of the effective magnetic attraction between polaritons, mediated by the ion subsystem.

DOI: 10.1103/PhysRevB.96.115310

I. INTRODUCTION

Exciton polaritons are versatile quantum quasiparticles that exist in semiconductor systems, in which the exciton-photon coupling overcomes the effects of decoherence [1]. This so-called strong-coupling regime is characterized by the appearance of new branches of excitations with mixed light-matter characteristics. In semiconductor microcavities, polaritonic modes possess an effective mass orders of magnitude smaller than the electron mass, which allows for the observation of bosonic condensation even at room temperature [2–4]. This led to the observation of phenomena such as superfluidity [5,6], Josephson oscillations [7,8], quantum vortices [9–11], and solitons [12–14]. The applications of polaritonic condensates that are considered currently include low threshold lasers [15], all-optical logic [16–18], quantum simulators [19,20] and few-photon sources [21].

Recently, exciton polaritons in semimagnetic (or diluted magnetic) semiconductor materials attracted increasing interest. In these materials, the response to magnetic field is enhanced by orders of magnitude due to the coupling of exciton spin to the spin of magnetic ions diluted in the semiconductor medium [22–26]. Recent progress in sample fabrication led to the observation of polariton lasing, or condensation, in a high-quality semimagnetic microcavity [27]. Importantly, and in contrast to standard semiconductor materials, the Zeeman energy splitting between polarized polariton lines can be very well resolved spectrally even at moderate magnetic fields [26,28]. This allows us to observe a number of qualitatively new physical phenomena. In particular, exciton polaritons have been proposed as a promising platform for topological quantum states in photonic lattices [29–34]. Unidirectional transport in topological states can be realized by breaking time-reversal symmetry. In the polariton context, this is possible thanks to the exciton sensitivity to the magnetic field [34].

One of the most fundamental phenomena predicted in condensates of semimagnetic polaritons is magnetic self-trapping [35], or the formation of magnetic polarons [36]. It was predicted that when the ion-exciton coupling is strong enough, and at low enough temperature, self-trapping can occur, which leads to condensation in real space and the breakdown of superfluidity [35]. However, this theoretical prediction was entirely based on the equilibrium model, in which condensation in the ground state of a system without dissipation was assumed. While an equilibrium condition in polariton condensates has been realized very recently in state-of-the-art GaAs microcavity samples [37], it is not satisfied in the majority of microcavities, and in particular $Cd_{1-x}Mn_xTe$ systems, which possess strong magnetic properties. It is therefore important to investigate the effect of the nonequilibrium nature of polariton condensates on the existence and properties of magnetic polarons.

In this paper, we investigate in detail magnetic self-trapping in polariton condensates while fully taking into account the nonequilibrium physics of the system. At the same time, we assume that the magnetic ion subsystem is fully thermalized, as evidenced in experiments [26]. We find that in the nonequilibrium case, multiple magnetic polarons can be formed at the same time, in contrast to previous findings [35]. We investigate both the case of homogeneous pumping with periodic boundary conditions, and a more realistic case of Gaussian pumping. Moreover, we find that the critical condition for self-trapping differs from the one predicted in equilibrium, as the polariton temperature cannot be defined. We obtain diagrams of stability as a function of the ion-polariton coupling, temperature, and magnetic field. Additionally, we use the Bogoliubov–de Gennes approximation to examine the stability of a uniform condensate against self-trapping. We derive an analytic formula for the stability threshold, which, surprisingly, does not depend on the spin relaxation time of the magnetic ions. These results are confirmed numerically and explained by the effective nonlinearity in the model. The self-trapping is directly connected to the effective magnetic attraction between polaritons, induced by the coupling to the ion subsystem.

II. MODEL

We consider an exciton-polariton condensate in a two-dimensional semimagnetic semiconductor microcavity. The cavity contains quantum wells that are composed of a diluted magnetic semiconductor (such as $Cd_{1-x}Mn_xTe$) with incorporated magnetic ions, a setup that has been realized recently [26,27]. We consider a specific case of a two-dimensional cavity where polaritons are confined in a one-dimensional

geometry by a microwire or line defect [38,39]. In this work, we will assume that the condensate is fully spin-polarized. This can be achieved experimentally by the combined effect of a circularly polarized pump, and the influence of an external magnetic field in the direction perpendicular to the quantum well, which suppresses an exciton spin-flip. We also neglect the effects of TE-TM splitting, which could lead to the precession of polariton spins in an effective magnetic field [40].

In the case of tight transverse confinement, the evolution of the condensate can be described by the complex Ginzburg-Landau equation (CGLE) coupled to the equation describing spin relaxation of magnetic ions [41],

$$i\hbar\frac{\partial\psi}{\partial t} = -\frac{\hbar^2}{2m^*}\frac{\partial^2\psi}{\partial x^2} + g_C|\psi|^2\psi - \gamma_{NL}|\psi|^2\psi - \lambda M\psi + iP(x)\psi - i\frac{1}{2}\gamma_L\psi, \quad (1)$$

$$\frac{\partial M(x,t)}{\partial t} = \frac{\langle M(x,t)\rangle - M(x,t)}{\tau_M}, \quad (2)$$

where g_C is the polariton interaction constant, γ_L and γ_{NL} are linear and nonlinear loss coefficients, respectively, λ is the magnetic ion-polariton coupling constant, τ_M is the spin relaxation time of magnetic ions, and $P(x)$ is the space-dependent external pumping rate. We note that the nonlinear coefficients have been rescaled in the one-dimensional (1D) case and are related to their 2D counterparts through $(g_C^{1D},\gamma_{NL}^{1D}) = (g_C^{2D},\gamma_{NL}^{2D})/\sqrt{2\pi d^2}$, where d is the length scale of the transverse confinement. Here, we assumed a Gaussian transverse profile of $|\psi|^2$ of width d. In the case of a one-dimensional microwire [38], the profile width d is of the order of the microwire thickness. We emphasize that the pumping and loss terms in Eq. (1) were absent in the previous study of magnetic self-trapping [35].

The equilibrium ion magnetization in the dilute regime is given by the Brillouin function [42]

$$\langle M(x,t)\rangle = n_M g_M \mu_B J B_J\left(\frac{g_M\mu_B J B_{eff}}{k_B T}\right), \quad (3)$$

where n_M and g_M are the 1D concentration and g-factor of magnetic ions with total spin $J = 5/2$, μ_B is the Bohr magneton, T is the ion subsystem temperature, and B_{eff} is an effective magnetic field that consists of an external magnetic field B_0 and a contribution from the interaction with the polarized condensate,

$$B_{eff} = B_0 + \tfrac{1}{2}\lambda|\psi|^2 = B_0 + \lambda S_z, \quad (4)$$

where S_z is the polariton 1/2-pseudospin density. Here, because of the assumption of full condensate polarization, S_z is simply equal to half of the polariton density $n = |\psi|^2/2$. The coupling constant λ can be estimated as [35]

$$\lambda = \frac{\beta_{ex}X^2}{\mu_B g_M L_z}, \quad (5)$$

where β_{ex} is the ion-exciton exchange interaction constant, X is the excitonic Hopfield coefficient, and L_z is the width of the quantum well.

We consider two cases of space dependence of the pumping profile $P(x)$, i.e., homogeneous and Gaussian pumping. In the case of uniform pumping, the effective pumping is simply the difference of pumping and linear loss terms, $P_{eff} = P - \gamma_L$. In the Gaussian pumping case, we assume

$$P(x) = P_1\exp\left(-\frac{x^2}{2\sigma_p^2}\right), \quad (6)$$

where σ_p corresponds to the spatial width of the pump beam.

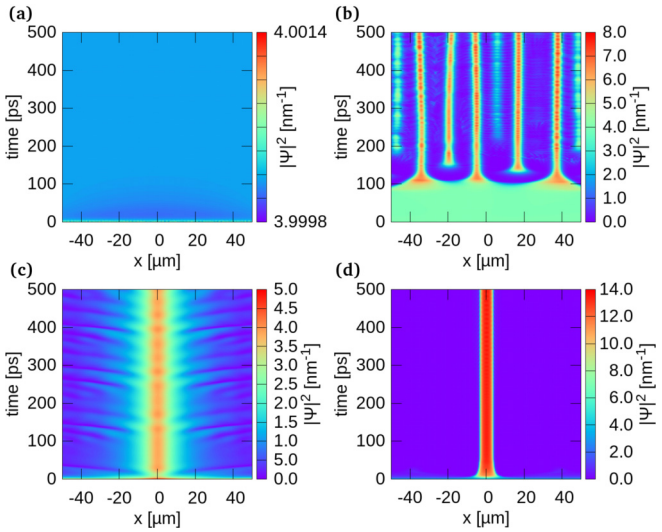

FIG. 1. Evolution of the norm $|\psi|^2$ of the condensate wave function. Upper plots show the case of uniform pumping; bottom plots show the case of Gaussian pumping. Left-hand plots show stable cases when $\lambda < \lambda_C$; right-hand plots show unstable cases in which polarons are formed. Parameters: $\gamma_L = 0$ meV in (a),(b); $\gamma_L = 6.582\times10^{-2}$ meV in (c),(d); $\lambda = 7.125\times10^{-12}$ T m in (a),(c); $\lambda = 8.125\times10^{-12}$ T m in (b); $\lambda = 9.5\times10^{-12}$ T m in (d). Others parameters are given in [43].

III. NUMERICAL RESULTS

It was demonstrated [35] that when the coupling between the polariton and magnetic subsystems is strong enough, self-trapping can occur due to the magnetic polaron effect [36,41]. The critical condition for self-trapping was given under the assumption of thermal equilibrium in the system. We note, however, that in the majority of current experiments, thermal equilibrium is not achieved. In contrast, condensation of exciton polaritons often takes place in far-from-equilibrium conditions, where it is driven by the system kinetics without a well-defined temperature of the polariton subsystem. It is therefore important to investigate what the influence is of the nonequilibrium character of polariton condensation on the magnetic polaron effect.

Before analyzing the precise conditions for self-trapping, we demonstrate examples of typical behavior of the system. In Fig. 1, we show examples of dynamics obtained from Eqs. (1) and (2) under both uniform and Gaussian pumping and at $B = 0$. The numerical space window was set to be $x \in (-100\ \mu\text{m}, 100\ \mu\text{m})$ with periodic boundary conditions, and the parameters correspond to a $Cd_{1-x}Mn_xTe$ sample with a few percent concentration of Mn ions. In the case of Gaussian pumping, absorbing boundary conditions were implemented

at the edges of the numerical grid. In all cases, the initial state was given by a homogeneous state ($n = |\psi_0|^2$) close to the stationary state of model equations, perturbed by a small white Gaussian noise.

Figures 1(a) and 1(b) correspond to the case of homogeneous pumping. At a lower value of the ion-exciton coupling constant λ, the homogeneous state given by the stationary condition $n = P_0/\gamma_{\mathrm{NL}}$ is stable, as shown in Fig. 1(a). However, when the coupling constant becomes higher than a certain threshold λ_c, the formation of localized polarons can be observed in Fig. 1(b). The polarons are almost stationary and surrounded by areas of very low polariton density. Some temporal oscillations of polaron widths can be seen. Polarons are characterized by both high polariton density and ion magnetization (not shown), which evidences the interaction between these subsystems.

In the case of a Gaussian pumping profile, below the critical threshold for self-trapping, a condensate is formed in the area covered by the pumping beam. As shown Fig. 1(c), it may also exhibit oscillations that are, however, not related to the polaron effect. Crossing the threshold λ_c leads to a dramatic reduction of the spatial size of the condensate, as shown in Fig. 1(d), in agreement with results obtained in [35].

The above examples are generic and correspond to dynamics occurring generally at various values of model parameters. Therefore, we conclude that the polaron self-trapping effect can be observed in a nonequilibrium condensate, although in contrast to a previous study [35], we find that multiple polarons can exist in the system at the same time, both in the case of homogeneous and Gaussian pumping. We investigated the parameter space of the model in a systematic way to determine the conditions for self-trapping in a nonequilibrium system. The phase diagram in the space of the coupling constant and the relaxation time for homogeneous pumping is shown in Fig. 2. Results of numerical simulations of model equations are indicated by crosses (stable condensate) and circles (self-trapping). Additionally, we show the results of Bogoliubov–de Gennes analysis of stability of the uniform state (see Sec. IV for details), which are given by the color scale. Clearly there is a very good agreement between the analytical predictions and the results of numerical simulations. One can observe that the coupling constant λ is the most important parameter that determines the stability, and τ_{M} only has an influence on the instability rate of the steady state, which corresponds to the time necessary for the formation of polarons. Interestingly, there exist two regions of stability for low and high values of λ. The upper region corresponds to the saturation of the magnetic response due to the shape of the Brillouin function. As will be shown below, the effective nonlinearity depends on the first derivative of B_J.

Figure 3 contains phase diagrams (according to the BdG stability analysis) in the space of the ion temperature T and ion-polariton coupling λ, at (a) zero magnetic field and (b) a magnetic field of 1 T. Note that (a) suggests that in the case of a low coupling constant, very low temperatures are necessary to observe the polaron effect. However, this dependence becomes less pronounced for higher values of λ. The main effect of the magnetic field exists at small temperatures, where the uniform condensate becomes stable for all values of λ.

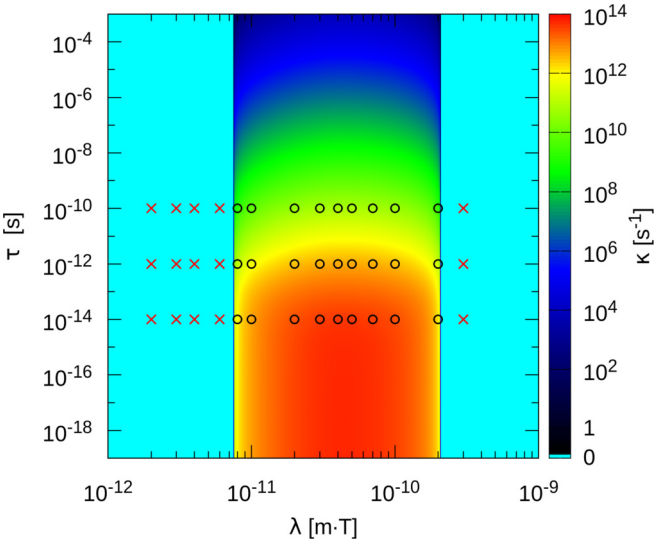

FIG. 2. Diagram of stability shown in coordinates of the ion-polariton coupling constant λ and the spin relaxation time of magnetic ions τ. Stability limits were calculated analytically (see Sec. IV). The color scale represents the instability rate according to the Bogoliubov–de Gennes approximation; cyan shows that the system is stable (it is symbolically expressed by "0" on the logarithmic scale); circles correspond to unstable states as predicted by the simulation of Eqs. (1) and (2); crosses correspond to stable states.

Finally, we note that the degree of circular polarization of the condensate depends, among other parameters, on the temperature and magnetic field, due to the existence of spin-flip processes. For this reason, in particular in the $B = 0$ case, the condensate can become polarized elliptically or linearly at low temperatures, which will lead to the modification of the phase diagram shown in Fig. 3(a).

IV. STABILITY ANALYSIS

In this section, we apply the Bogoliubov–de Gennes approximation in the case of uniform pumping to find an analytical condition of stability of a stationary state. We postulate that the emergence of magnetic polarons corresponds to the instability threshold for the uniform state. Indeed, we find a full analogy of the effective nonlinearity emerging from the model Eqs. (1) and (2) in the fast relaxation rate regime to the Gross-Pitaevskii equation with attractive nonlinearity. In terms of this correspondence, polarons can be identified as bright solitons emerging from an unstable uniform background [44].

For the sake of clarity of the derivation, we now introduce a dimensionless form of the model. Equations (1) and (2) can be transformed by rescaling time, space, wavefunction amplitude, and system parameters as $t = \alpha\tilde{t}$, $x = \xi\tilde{x}$, $\psi = (\xi\beta)^{-1/2}\tilde{\psi}$, $g_{\mathrm{C}} = \hbar\xi\beta\alpha^{-1}\tilde{g_{\mathrm{C}}}$, $P_{\mathrm{eff}} = \hbar\alpha^{-1}\tilde{P}$, $\gamma_{\mathrm{NL}} = \hbar\xi\beta\alpha^{-1}\tilde{\gamma_{\mathrm{NL}}}$, $M = \zeta\tilde{M}$, and $\lambda = \hbar\alpha^{-1}\tilde{\lambda}$ to obtain the dimensionless form (hereafter we omit the tildes)

$$i\frac{\partial\psi}{\partial t} = -\frac{\partial^2\psi}{\partial x^2} + g_{\mathrm{C}}|\psi|^2\psi + iP\psi - i\gamma_{\mathrm{NL}}|\psi|^2\psi - \zeta\lambda M\psi \tag{7}$$

$$\frac{\partial M}{\partial t} = \frac{\alpha}{\tau_{\mathrm{M}}}[JB_J(\delta\lambda|\psi|^2) - M], \tag{8}$$

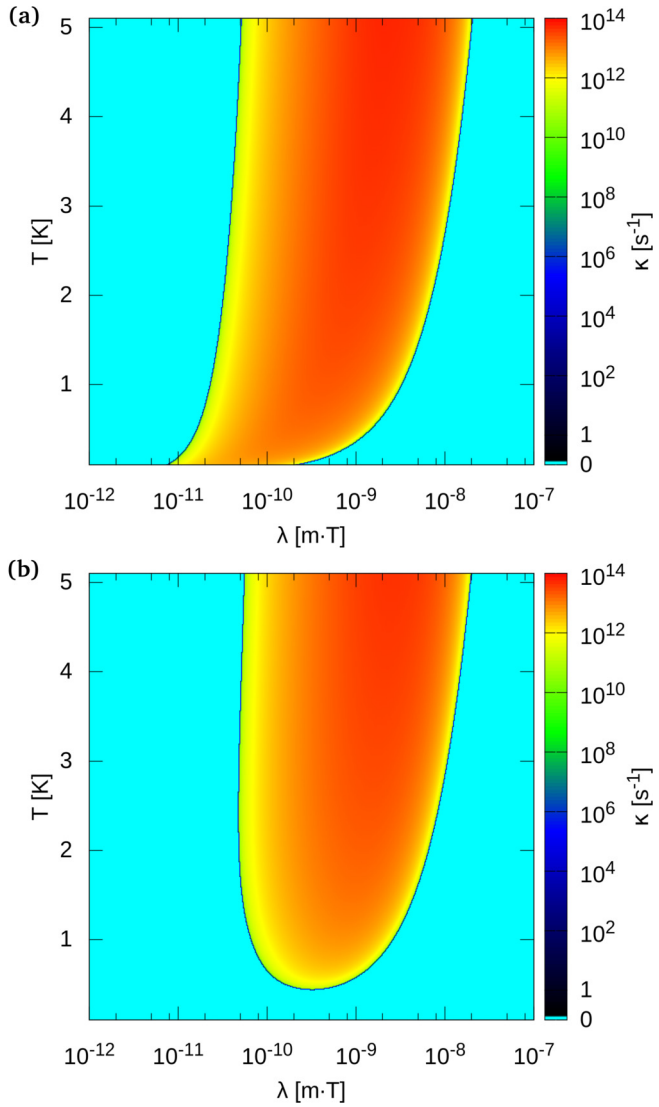

FIG. 3. Diagrams of stability shown in coordinates of the ion-polariton coupling constant λ and temperature T. (a) The case without magnetic field; (b) the case with a magnetic field of $B = 1$ T. Color code and parameters are the same as in Fig. 2 and the spin relaxation time is $\tau = 10^{-12}$ s.

where $\xi = \sqrt{\hbar\alpha/2m^*}$, $\zeta = g_M\mu_B n_M$, $\delta = \frac{g_M\mu_B J}{2k_B T}\frac{\hbar}{\alpha\beta\xi}$, and α,β are free parameters.

Fluctuation around the stationary homogeneous solution $\psi_0(x,t) = n^{1/2}e^{-i\mu t}$, $M_0(x,t) = JB_J(\delta\lambda|\psi_0|^2)$ can be written in the plane-wave basis [45] (note that $n = P/\gamma_{NL}$)

$$\psi(x,t) = n^{1/2}e^{-i\mu t}\left[1 + \epsilon\sum_k\{u_k(t)e^{ikx} + v_k(t)e^{-ikx}\}\right], \tag{9}$$

$$M(x,t) = M_0 + \epsilon\sum_k[w_k(t)e^{ikx} + w_k^*(t)e^{-ikx}], \tag{10}$$

where ϵ is a small perturbation parameter.

The linearized solution is obtained by taking ϵ up to the first order, expanding the Brillouin function about ψ_0 up to the first term, and comparing parts with e^{ikx} and e^{-ikx}, respectively. It can be rewritten as the following eigenvalue problem:

$$i\frac{d}{dt}\begin{pmatrix}u\\ v^*\\ w\end{pmatrix} = Q\begin{pmatrix}u\\ v^*\\ w\end{pmatrix}, \tag{11}$$

where the matrix Q is given by

$$Q = \begin{pmatrix} k^2 - iEn + g_C n & -iEn + g_C n & -\zeta\lambda n^{1/2} \\ -iEn - g_C n & -k^2 - iEn - g_C n & \zeta\lambda n^{1/2} \\ i\frac{\alpha}{\tau}\delta\lambda n^{1/2}JB_J'(\delta\lambda n) & i\frac{\alpha}{\tau}\delta\lambda n^{1/2}JB_J'(\delta\lambda n) & -i\frac{\alpha}{\tau}\end{pmatrix}. \tag{12}$$

The numerical solution of the above eigenvalue problem in parameter space is shown in Figs. 2 and 3 in a color scale, which corresponds to the most unstable mode (highest imaginary part of the eigenfrequency) of the system (11). Parameters with stable evolution (all eigenvalues with a zero or negative imaginary part) are depicted by a cyan color.

Additionally, it is possible to derive an exact analytical condition for the stability of the system. The procedure is analogous to the one described in [46] and consists of the analysis of the zero-frequency crossing of the imaginary part of the eigenfrequency as a function of momentum k. The existence of the crossing indicates that momenta with eigenfrequencies with both positive and negative imaginary parts exist on two sides of the crossing. The eigenvalue problem of Eq. (12) leads to the equation for $\omega(k)$,

$$\omega^3 + i(Y + 2R)\omega^2 - \left(\omega_B^2 + 2YR\right)\omega = iY\left(\omega_B^2 - 2Gk^2\right), \tag{13}$$

where ω_B, Y, R, and G are defined by

$$\omega_B^2 = k^4 + 2k^2 g_C n, \tag{14}$$

$$Y = \frac{\alpha}{\tau},\ R = En,\ G = \zeta\delta\lambda^2 JB_J'(\delta\lambda n)n. \tag{15}$$

We can analyze the solutions in the limits $k \to \infty$ and $k \to 0$. In the $k \to \infty$ limit, there are three branches: $\omega \approx -iY, \pm k^2 - iR$, and all have negative imaginary parts. In the $k \to 0$ limit, there are two solutions with negative imaginary parts and one equal to zero: $\omega_1(0) = 0$, $\omega_2(0) = -iY$, and $\omega_3(0) = -2iR$. Only the ω_1 branch can cross the zero-frequency axis and have a positive imaginary part in some range of k. The crossing points can be found by putting $\mathrm{Im}(\omega) = 0$ and $\mathrm{Re}(\omega) = \Omega$ into Eq. (13), which have to be satisfied at the same time,

$$\Omega\left[\Omega^2 - \left(\omega_B^2 + 2YR\right)\right] = 0, \tag{16}$$

$$(Y + 2R)\Omega - Y\omega_B^2 + 2YGk^2 = 0. \tag{17}$$

For physical parameters, Eqs.(16) and (17) are realized only if $\Omega = 0$. That leads to the equation for k,

$$k^4 + 2k^2 g_C n + 2Gk^2 = 0, \tag{18}$$

and the analytical condition for stability, which expressed in physical units reads

$$\lambda^2 B_J'\left(\frac{g_M\mu_B}{2k_BT}\lambda n J\right) < \frac{2g_C k_B T}{n_M g_M^2 \mu_B^2 J^2}. \quad (19)$$

With respect to λ, the inequality (19) is not satisfied in the interval $\lambda_{c1} < \lambda < \lambda_{c2}$, as can be seen in Fig. 2. Remarkably, the critical values of λ do not depend on the spin relaxation time τ. This conclusion is fully supported by the numerical simulations as shown in Fig. 2. In this figure, the color scale shows the calculated largest eigenvalue of the unstable branch, $\kappa = \max(\mathrm{Im}\,\omega_1(k))$. Parameters for which $\mathrm{Im}\,\omega_1(k)$ is always nonpositive are marked by a cyan color.

A. Adiabatic regime

As is shown in Fig. 2, if the ion spin relaxation time τ is shorter than 10^{-14} s, the instability rate no longer depends on the value of τ. In this adiabatic regime, the fast spin relaxation approximation can be applied, which corresponds to setting the time derivative on the left-hand side of Eq. (8) to zero. In this limit, we have $M(x,t) = \langle M(x,t)\rangle = J B_J(\delta\lambda|\psi|^2)$, which gives

$$i\frac{\partial\psi}{\partial t} = -\frac{\partial^2\psi}{\partial x^2} + [g_C|\psi|^2 - \zeta\lambda\langle M(x,t)\rangle]\psi - i(\gamma_{NL}|\psi|^2 - P)\psi. \quad (20)$$

A simple and intuitive interpretation of the instability can be obtained if the Brillouin function is expanded up to first order around the stationary value of $|\psi_0|^2$,

$$M(x,t) = J B_J(\delta\lambda|\psi|^2) \approx J B_J(\delta\lambda|\psi_0|^2) + J\delta\lambda(|\psi|^2 - |\psi_0|^2)B_J'(\delta\lambda|\psi_0|^2), \quad (21)$$

which leads to the standard form of the complex Ginzburg-Landau equation (or dissipative Gross-Pitaevskii equation),

$$i\frac{\partial\psi}{\partial t} = -\frac{\partial^2\psi}{\partial x^2} + [(g_C - \zeta\lambda^2\delta B_J')|\psi|^2 - \zeta\lambda U_0]\psi - i(\gamma_{NL}|\psi|^2 - P)\psi, \quad (22)$$

where $U_0 = J B_J(\delta\lambda|\psi_0|^2) - J\delta\lambda|\psi_0|^2 B_J'(\delta\lambda|\psi_0|^2)$ and the notation $B_J' = B_J'(\delta\lambda|\psi_0|^2)$ was used. The above form corresponds to the complex Ginzburg-Landau equation with effective nonlinearity,

$$g_{eff} = g_C - J\zeta\lambda^2\delta B_J', \quad (23)$$

which becomes attractive exactly at the threshold given by Eq. (19) when expressed in physical units. In other words, the instability threshold that marks the formation of polarons corresponds to the Benjamin-Feir-Newell criterion of stability of the CGLE equation [47].

B. Quasiparticle spectrum

Figure 4 shows the imaginary part of the excitation spectrum of the uniformly pumped condensate. Figure 4(a) is an example of weak instability in the case of a long ion spin relaxation rate, which corresponds to circles in the green area in Fig. 2. The spectrum contains three branches, of which one (blue line) is unstable at a certain wave-vector range, which is indicated by the positive imaginary part of the frequency. We note that the spectrum in this regime is strikingly similar to the one predicted in the case of a nonmagnetic condensate in the presence of a reservoir [45,48]. The similarity indicates that the magnetic ions play in some sense the role of a reservoir in this system.

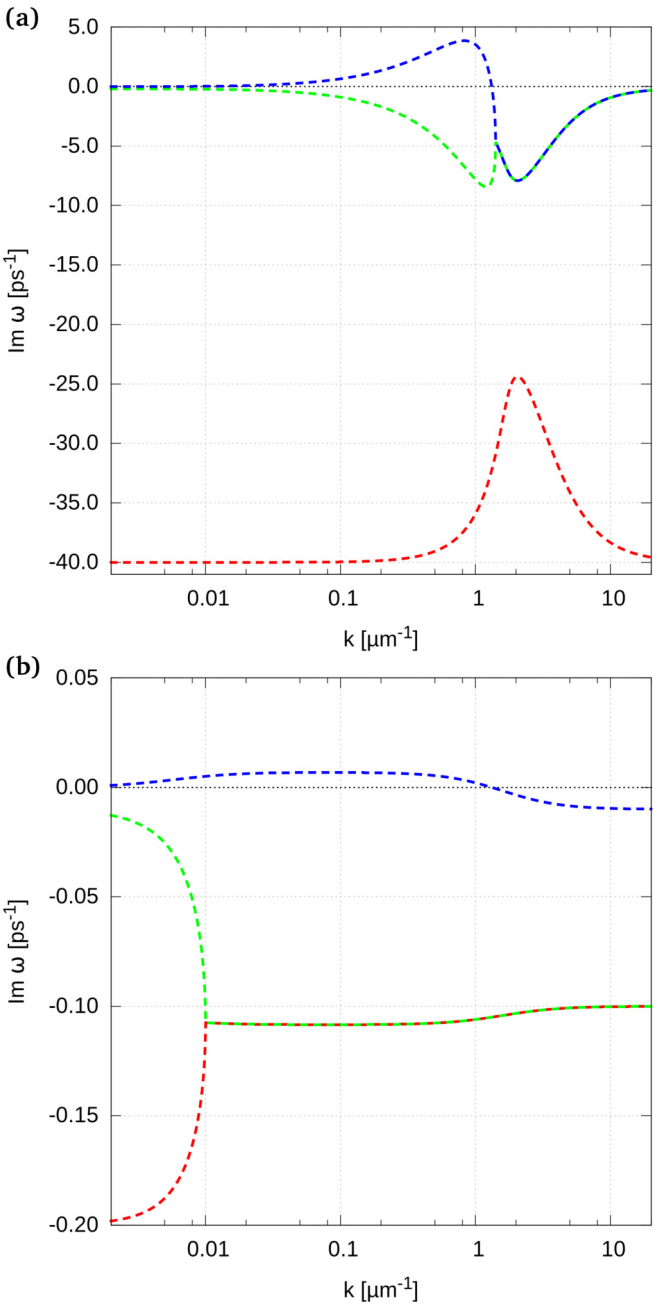

FIG. 4. Imaginary parts of the frequencies of Bogoliubov quasiparticles. The ion-polariton coupling constant λ is 10^{-11} T m. (a) A typical excitation spectrum; spin relaxation time $\tau = 10^{-10}$ s. The unstable branch exhibits a positive imaginary part. (b) Large instability rate at $\tau = 2.5 \times 10^{-14}$ s.

On the other hand, in the case of a short spin relaxation time, the spectrum becomes qualitatively different, as indicated in Fig. 4(b). These parameters correspond to circles in the orange

area of Fig. 2. While one of the branches is also unstable, it is strongly peaked at high momenta. Moreover, the instability rate, defined as the maximum value of the imaginary part of the frequency, is much higher than in the previous case. This indicates clearly that the relaxation time determines the time scale of the instability, as demonstrated in Fig. 2. The lower branch (red line) has been pushed down to very low imaginary frequencies, which is characteristic of a strongly damped mode. This damped mode is the one that corresponds to the excitation of magnetization, which is strongly suppressed in the adiabatic regime.

V. CONCLUSIONS

In conclusion, we investigated a spin-polarized condensate of exciton polaritons in a diluted magnetic semiconductor microcavity. In contrast to previous works, we included nonequilibrium effects of driving and decay in our model, which led to several interesting effects. We found that multiple polarons can exist at the same time, and we connected the instability of the homogeneous state in the Bogoliubov–de Gennes approximation to the formation of polarons. We derived a critical condition for self-trapping that is different from the one predicted previously in the equilibrium case. The effect has been explained by the effective attraction between polaritons due to magnetic ion coupling.

Experimentally, it is important to distinguish magnetic self-trapping from trapping on defects existing in the sample. Such localization is routinely observed in experiments with condensates in a strong disorder potential [2]. This effect could prevent the observation of self-trapping if the disorder energy scale is larger than the strength of nonlinearity. As the disorder is typically significant in CdTe samples considered here, it is important to make sure that the samples used are characterized by a disorder that does not prevent the observation of self-trapping. Recent advances in sample fabrication should allow this regime to be reached [27]. Additionally, the nonlinear self-trapping effect is predicted to become more significant at large polariton densities, in contrast to trapping in defects, which is typically the strongest at low pumping powers.

ACKNOWLEDGMENT

We acknowledge support from the National Science Center Grants No. 2015/17/B/ST3/02273 and No. 2016/22/E/ST3/00045. We thank Alexey Kavokin, Barbara Pietka and Jacek Szczytko for useful discussions.

[1] J. J. Hopfield, Phys. Rev. **112**, 1555 (1958); C. Weisbuch, M. Nishioka, A. Ishikawa, and Y. Arakawa, Phys. Rev. Lett. **69**, 3314 (1992); A. V. Kavokin, J. J. Baumberg, G. Malpuech, and F. P. Laussy, *Microcavities* (Oxford University Press, Oxford, 2007).

[2] J. Kasprzak, M. Richard, S. Kundermann, A. Baas, P. Jeambrun, J. M. J. Keeling, F. M. Marchetti, M. H. Szymańska, R. André, J. L. Staehli *et al.*, Nature (London) **443**, 409 (2006).

[3] S. Christopoulos, G. B. H. von Högersthal, A. J. D. Grundy, P. G. Lagoudakis, A. V. Kavokin, J. J. Baumberg, G. Christmann, R. Butté, E. Feltin, J.-F. Carlin *et al.*, Phys. Rev. Lett. **98**, 126405 (2007).

[4] K. S. Daskalakis, S. A. Maier, and R. M. S. Kena-Cohen, Nat. Mater. **13**, 271 (2014).

[5] A. Amo, J. Lefrère, S. Pigeon, C. Adrados, C. Ciuti, I. Carusotto, R. Houdré, E. Giacobino, and A. Bramati, Nat. Phys. **5**, 805 (2009).

[6] G. Lerario, A. Fieramosca, F. Barachati, D. Ballarini, K. S. Daskalakis, L. Dominici, M. De Giorgi, S. A. Maier, G. Gigli, S. Kéna-Cohen, and D. Sanvitto, Nat. Phys. (2017), doi: 10.1038/nphys4147.

[7] K. G. Lagoudakis, B. Pietka, M. Wouters, R. André, and B. Deveaud-Plédran, Phys. Rev. Lett. **105**, 120403 (2010).

[8] M. Abbarchi, A. Amo, V. G. Sala, D. D. Solnyshkov, H. Flayac, L. Ferrier, I. Sagnes, E. Galopin, A. Lemaître, G. Malpuech, and J. Bloch, Nat. Phys. **9**, 275 (2013).

[9] K. G. Lagoudakis, M. Wouters, M. Richard, A. Baas, I. Carusotto, R. André, L. S. Dang, and B. Deveaud-Plédran, Nat. Phys. **4**, 706 (2008).

[10] D. Sanvitto, F. M. Marchetti, M. H. Szymańska, G. Tosi, M. Baudisch, F. P. Laussy, D. N. Krizhanovskii, M. S. Skolnick, L. Marrucci, A. Lemaître, J. Bloch, C. Tejedor, and L. Viña, Nat. Phys. **6**, 527 (2010).

[11] K. G. Lagoudakis, F. Manni, B. Pietka, M. Wouters, T. C. H. Liew, V. Savona, A. V. Kavokin, R. André, and B. Deveaud-Plédran, Phys. Rev. Lett. **106**, 115301 (2011).

[12] A. Amo, S. Pigeon, D. Sanvitto, V. G. Sala, R. Hivet, I. Carusotto, F. Pisanello, G. Leménager, R. Houdré, E. Giacobino, C. Ciuti, and A. Bramati, Science **332**, 1167 (2011).

[13] M. Sich, D. N. Krizhanovskii, M. S. Skolnick, A. V. Gorbach, R. Hartley, D. V. Skryabin, E. A. Cerda-Méndez, K. Biermann, R. Hey, and P. V. Santos, Nat. Photon. **6**, 50 (2012).

[14] L. Dominici, M. Petrov, M. Matuszewski, D. Ballarini, M. De Giorgi, D. Colas, E. Cancellieri, B. S. Fernandez, A. Bramati, G. Gigli, A. Kavokin, F. Laussy, and D. Sanvitto, Nat. Commun. **6**, 8993 (2015).

[15] T. Byrnes, N. Y. Kim, and Y. Yamamoto, Nat. Phys. **10**, 803 (2014).

[16] D. Ballarini, M. De Giorgi, E. Cancellieri, R. Houdré, E. Giacobino, R. Cingolani, A. Bramati, G. Gigli, and D. Sanvitto, Nat. Commun. **4**, 1778 (2013).

[17] T. Gao, P. S. Eldridge, T. C. H. Liew, S. I. Tsintzos, G. Stavrinidis, G. Deligeorgis, Z. Hatzopoulos, and P. G. Savvidis, Phys. Rev. B **85**, 235102 (2012).

[18] T. C. H. Liew, A. V. Kavokin, and I. A. Shelykh, Phys. Rev. Lett. **101**, 016402 (2008).

[19] N. G. Berloff, K. Kalinin, M. Silva, W. Langbein, and P. G. Lagoudakis, arXiv:1607.06065.

[20] N. Y. Kim and Y. Yamamoto, in *Quantum Simulations with Photons and Polaritons* (Springer, New York, 2017), pp. 91–121.

[21] C. S. Muñoz, E. D. Valle, A. G. Tudela, K. Müller, S. Lichtmannecker, M. Kaniber, C. Tejedor, J. J. Finley, and F. P. Laussy, Nat. Photon. **8**, 550 (2014).

[22] *Diluted Magnetic Semiconductors*, edited by J. K. Furdyna and J. Kossut, Semiconductors and Semimetals (Academic, New York, 1988), Vol. 25.

[23] T. Dietl, *(Diluted) Magnetic Semiconductors*, in *Handbook on Semiconductors*, 2nd ed., Vol. 3B, *Materials, Properties and Preparations*, edited by S. Mahajan (North-Holland, Amsterdam, 1994).

[24] E. L. Ivchenko, A. V. Kavokin, V. P. Kochereshko, G. R. Posina, I. N. Uraltsev, D. R. Yakovlev, R. N. Bicknell-Tassius, A. Waag, and G. Landwehr, Phys. Rev. B **46**, 7713 (1992).

[25] A. Brunetti, M. Vladimirova, D. Scalbert, R. André, D. Solnyshkov, G. Malpuech, I. A. Shelykh, and A. V. Kavokin, Phys. Rev. B **73**, 205337 (2006).

[26] R. Mirek, M. Król, K. Lekenta, J.-G. Rousset, M. Nawrocki, M. Kulczykowski, M. Matuszewski, J. Szczytko, W. Pacuski, and B. Pietka, Phys. Rev. B **95**, 085429 (2017).

[27] J.-G. Rousset, B. Pietka, M. Król, R. Mirek, K. Lekenta, J. Szczytko, J. Borysiuk, J. Suffczyński, T. Kazimierczuk, M. Goryca, T. Smoleński, P. Kossacki, M. Nawrocki, and W. Pacuski, Appl. Phys. Lett. **107**, 201109 (2015).

[28] B. Pietka, D. Zygmunt, M. Król, M. R. Molas, A. A. L. Nicolet, F. Morier-Genoud, J. Szczytko, J. Lusakowski, P. Zieba, I. Tralle, P. Stepnicki, M. Matuszewski, M. Potemski, and B. Deveaud, Phys. Rev. B **91**, 075309 (2015).

[29] L. Lu, J. D. Joannopoulos, and M. Soljacic, Nat. Phys. **12**, 626 (2016).

[30] C.-E. Bardyn, T. Karzig, G. Refael, and T. C. H. Liew, Phys. Rev. B **91**, 161413 (2015).

[31] M. Milicevic, T. Ozawa, P. Andreakou, I. Carusotto, T. Jacqmin, E. Galopin, A. Lemaître, L. L. Gratiet, I. Sagnes, J. Bloch, and A. Amo, 2D Mater. **2**, 034012 (2015).

[32] F. Baboux, E. Levy, A. Lemaître, C. Gómez, E. Galopin, L. Le Gratiet, I. Sagnes, A. Amo, J. Bloch, and E. Akkermans, Phys. Rev. B **95**, 161114 (2017).

[33] A. V. Nalitov, D. D. Solnyshkov, and G. Malpuech, Phys. Rev. Lett. **114**, 116401 (2015).

[34] D. Solnyshkov, G. Malpuech, C. R. Phys. **17**, 920 (2016).

[35] I. A. Shelykh, T. C. H. Liew, and A. V. Kavokin, Phys. Rev. B **80**, 201306(R) (2009).

[36] T. Dietl and J. Spalek, Phys. Rev. Lett. **48**, 355 (1982).

[37] Y. Sun, P. Wen, Y. Yoon, G. Liu, M. Steger, L. N. Pfeiffer, K. West, D. W. Snoke, and K. A. Nelson, Phys. Rev. Lett. **118**, 016602 (2017).

[38] E. Wertz, L. Ferrier, D. D. Solnyshkov, R. Johne, D. Sanvitto, A. Lemaître, I. Sagnes, R. Grousson, A. V. Kavokin, P. Senellart *et al.*, Nat. Phys. **6**, 860 (2010).

[39] F. Manni, K. G. Lagoudakis, B. Pietka, L. Fontanesi, M. Wouters, V. Savona, R. André, and B. Deveaud-Plédran, Phys. Rev. Lett. **106**, 176401 (2011).

[40] I. A. Shelykh, Y. G. Rubo, G. Malpuech, D. D. Solnyshkov, and A. Kavokin, Phys. Rev. Lett **97**, 066402 (2006).

[41] A. Kavokin, B. Gil, and P. Bigenwald, Phys. Rev. B **57**, R4261 (1998).

[42] J. A. Gaj, R. Planel, and G. Fishman, Solid State Commun. **29**, 435 (1979).

[43] $n = 4 \times 10^9\,\mathrm{m}^{-1}$, $\tau = 10^{-12}\,\mathrm{ps}$, $g_\mathrm{C} = 1.2 \times 10^{-9}\,\mathrm{meV\,m}$, $n_\mathrm{M} = 10^{13}\,\mathrm{m}^{-1}$, $B = 0\mathrm{T}$, $T = 0.1\mathrm{K}$, $\gamma_\mathrm{NL} = 1.646 \times 10^{-11}\,\mathrm{meV\,m}$, $P_0 = 0.0658\mathrm{meV}$, $P_1 = 0.2633\mathrm{meV}$, $\sigma_p = 3.617 \times 10^{-6}\,\mathrm{m}$, $d = 8 \times 10^{-7}\,\mathrm{m}$. There was 5 meV Rabi splitting and zero-photon–exciton detuning; photon effective mass $m_\mathrm{C} = 10^{-5} m_\mathrm{E}$ and exciton effective mass $m_\mathrm{X} = 0.22 m_\mathrm{E}$.

[44] Y. S. Kivshar and G. P. Agrawal, *Optical Solitons, From Fibers to Photonic Crystals* (Academic, New York, 2003).

[45] M. Wouters and I. Carusotto, Phys. Rev. Lett. **99**, 140402 (2007).

[46] L. A. Smirnov, D. A. Smirnova, E. A. Ostrovskaya, and Y. S. Kivshar, Phys. Rev. B **89**, 235310 (2014).

[47] I. S. Aranson and L. Kramer, Rev. Mod. Phys. **74**, 99 (2002).

[48] N. Bobrovska, E. A. Ostrovskaya, and M. Matuszewski, Phys. Rev. B **90**, 205304 (2014).